

Anomalous length scaling of carbon nanotube-metal contact resistance: An ab initio study

Yong-Hoon Kim and Hu Sung Kim

Citation: *Appl. Phys. Lett.* **100**, 213113 (2012); doi: 10.1063/1.4721487

View online: <http://dx.doi.org/10.1063/1.4721487>

View Table of Contents: <http://apl.aip.org/resource/1/APPLAB/v100/i21>

Published by the [American Institute of Physics](http://www.aip.org).

Related Articles

A unified model for insulator selection to form ultra-low resistivity metal-insulator-semiconductor contacts to n-Si, n-Ge, and n-InGaAs

Appl. Phys. Lett. **101**, 042108 (2012)

Effect of metals and annealing on specific contact resistivity of GeTe/metal contacts

Appl. Phys. Lett. **101**, 012107 (2012)

Silicon fab-compatible contacts to n-InP and p-InGaAs for photonic applications

Appl. Phys. Lett. **100**, 201103 (2012)

Electrical contact resistance in filaments

Appl. Phys. Lett. **100**, 193115 (2012)

Observation of negative contact resistances in graphene field-effect transistors

J. Appl. Phys. **111**, 084314 (2012)

Additional information on *Appl. Phys. Lett.*

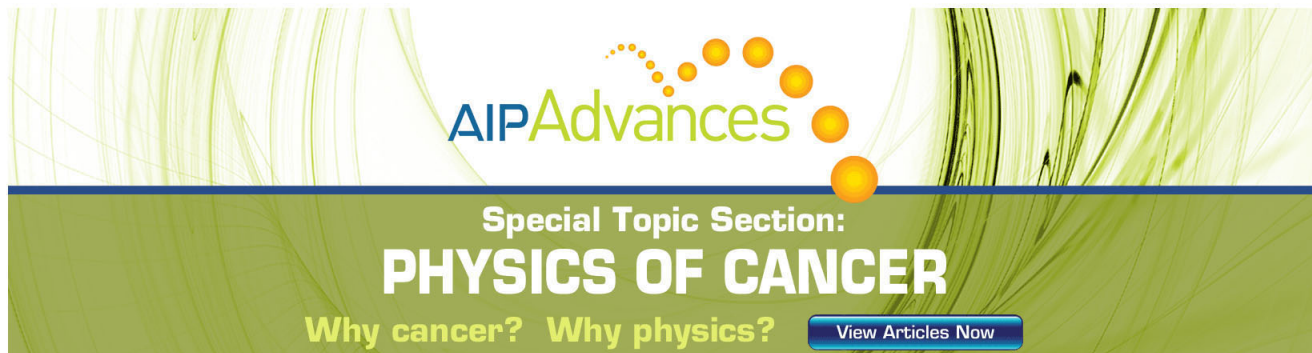
Journal Homepage: <http://apl.aip.org/>

Journal Information: http://apl.aip.org/about/about_the_journal

Top downloads: http://apl.aip.org/features/most_downloaded

Information for Authors: <http://apl.aip.org/authors>

ADVERTISEMENT



AIP Advances

Special Topic Section:
PHYSICS OF CANCER

Why cancer? Why physics? [View Articles Now](#)

Anomalous length scaling of carbon nanotube-metal contact resistance: An *ab initio* study

Yong-Hoon Kim (김용훈)^{a)} and Hu Sung Kim (김후성)

Graduate School of EEWS and KI for NanoCentury, Korea Advanced Institute of Science and Technology, Daejeon 305-701, South Korea

(Received 12 March 2012; accepted 9 May 2012; published online 24 May 2012)

Employing open-ended carbon nanotubes (CNTs) with and without hydrogen termination, we study the length scaling of metal-CNT contact resistance and its correlation with chemical bonding from first principles. Both models similarly show a transition from the fast-growing short-length scaling to the slow-growing long-length scaling. However, while the hydrogenated CNTs have much *lower* short-length resistances than H-free CNTs, Schottky barrier of the former is almost twice thicker and its eventual long-length-limit resistance becomes significantly *higher*. This demonstrates the critical role of atomistic details in metal-CNT contacts and localized CNT edge states for the Schottky barrier shape and metal-induced gap states. © 2012 American Institute of Physics. [<http://dx.doi.org/10.1063/1.4721487>]

While carbon nanotubes (CNTs) have long been considered as a prime candidate for next-generation field-effect transistor channel materials,^{1,2} achieving CNT transistors with dimensions suitable for future technology nodes still remains a paramount challenge.^{3,4} One of the major obstacles arises from the incomplete understanding and thus a guideline of atomic scale control of CNT-metal contacts.⁵ The device function of CNT transistors operating near the ballistic transport regime arises via the modulation of Schottky barriers at the metal-CNT interfaces rather than the channel conductance.⁶ However, the nature of Schottky barriers depends, in a complicated manner, on the CNT diameter, electrode metal type, and CNT-metal interface geometry,⁷ and there still exist large discrepancies in both theoretical predictions and experimental results.⁵ In fact, there is no agreement even on the optimal type of metal-CNT chemical bonding necessary to achieve low-resistance contacts. Most experimental efforts have focused on establishing strong metal-CNT chemical bonds.^{3,4} Meanwhile, it was also theoretically suggested that weak hybridization is ideal to form a “good” (low-Schottky barrier) contact.⁸

In this work, by carrying out large-scale first-principles calculations on two (10,0) CNT models with and without H edge termination contacted to Al(111) electrodes, we study the correlation between metal-CNT contact atomic structures and junction resistances. In a previous work, we have established the significant impact of CNT diameter on the contact resistances using (8,0) and (10,0) CNTs with H-free clean edges sandwiched between Au(111) electrodes. The key consideration point in the present study is, in addition to the strength of metal-CNT bonding, the scaling of resistance with nanotube length. We find that in both junction models the length scaling changes from a Schottky-barrier-dominated short-length scaling to a CNT-body-intrinsic long-length scaling. In spite of the similar transitioning behavior, we show that the channel length where the scaling transition occurs (i.e., twice the Schottky barrier width) is almost two times shorter for the contact model based on H-free CNTs.

So, although the contact resistance of the hydrogenated CNT (with weak metal-CNT chemical bonds) is, e.g., two orders of magnitude *lower* than that of the H-free CNT (with strong metal-CNT chemical bonds) at the channel length of about 2 nm, it eventually becomes about two orders of magnitude *higher* in the long channel length limit. The nontrivial and drastically different length scaling of junction resistances with the two similar contact models and especially the reversal of their ordering in the short and long length limits not only demonstrate the critical effect of atomistic details on contact resistances but also identify a source of contradicting theoretical predictions on the nature of metal-CNT chemical bonding that minimizes contact resistances—a key unresolved issue for the successful realization of carbon nanoelectronics. We will point out that the microscopic origin of the anomalous resistance length scaling behavior is the characteristic localized states in the CNT edges,^{9,10} which indicates that similar observations might be also made in graphene-based contacts.

In Fig. 1(a), we first show the open-ended CNT models without (**open**) and with (**H-end**) hydrogen termination adopted in this work. We used (10,0) CNT with diameter 0.79 nm, because smaller-diameter CNTs have work functions that substantially fluctuate with diameter¹¹ and accordingly non-general metal-CNT band alignment and charge injection properties.¹² The **open** model is typically employed for the first-principles study of contacts based on strong metal-CNT chemical bonds.^{12–15} On the other hand, the **H-end** model represents the weak metal-CNT chemical bonding situation. The length scaling of the side-contacted junction model, which is another widely used atomistic junction model with weak metal-CNT chemical bonds,^{8,15–19} is more difficult to consider from first principles as the contact length can be another important variable.⁴ While we leave it for future studies, we note that there exists evidence that the CNT edge is the more preferable charge injection path than the CNT side.^{20,21} The device models were finalized by sandwiching the **open** and **H-end** CNTs between two-layer 6 × 6 Al(111) slabs. The Al-CNT contact distance was fixed at 2.5 Å, which is between the optimal values for the two

^{a)}Electronic mail: y.h.kim@kaist.ac.kr.

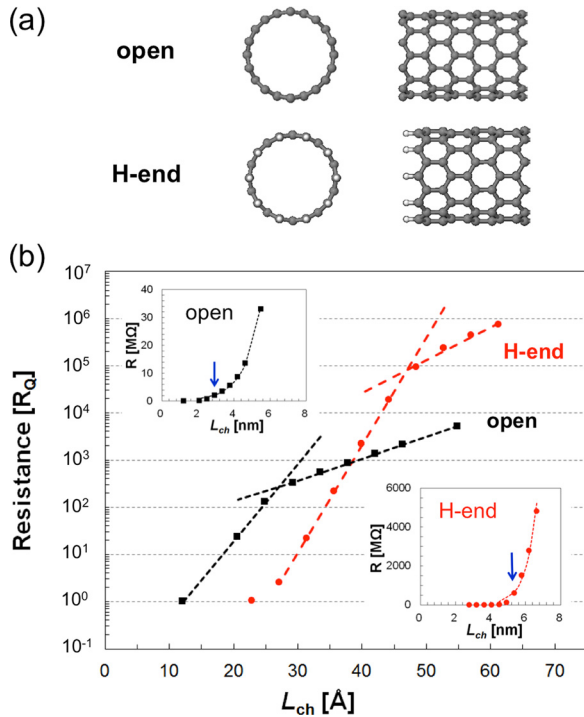


FIG. 1. (a) Top and side views of (10,0) CNT models without (**H-end**) and with (**open**) H termination employed in this work. (b) Resistance length scaling of the **open** (black squares) and **H-end** (red circles) models. Insets: The same curves shown in the normal scale together with the fits to the long-length scaling regimes starting at the transition points marked by arrows.

models, 2.0 Å for **open** and 3.3 Å for **H-end**. This enables a straightforward comparison of the charge injection capacity of the two cases without the complication of the contact-distance dependence. Results at the optimal contact distances will amplify the differences between the two models and not modify the results presented below in a qualitative manner.

We applied a first-principles approach combining density-functional theory (DFT) and matrix Green's function (MGF) calculations.^{12,22} Density functional calculations within the Perdew-Burke-Ernzerhof generalized-gradient approximation²³ were carried out using the SeqQuest program (Sandia National Laboratories), which is based on norm-conserving pseudopotentials and Gaussian basis sets. To extract the junction resistance information, we employed our in-house code that implements the MGF approach²⁴ and has been successfully applied to various systems including the metal-CNT contacts.^{12,22,25} We started from the device DFT calculations, for which we adopted the double- ζ -plus-polarization-level basis sets for aluminium and hydrogen and the single- ζ -level basis set and carbon. Next, transmission function was calculated according to

$$T(E) \equiv \text{Tr}[\Gamma_1(E)G(E)\Gamma_2(E)G^+(E)], \quad (1)$$

where G and Γ are the retarded Green's function, $G(E) = (ES - H + \Sigma_1 + \Sigma_2)^{-1}$, and broadening function, $\Gamma_{1,2} = i(\Sigma_{1,2} - \Sigma_{1,2}^+)$, respectively. The self-energies $\Sigma_{1/2}$ provide the *ab initio* broadening and shift of the channel energy levels attributed to the coupling between the CNTs and metal electrode 1/2. The surface green functions, a key ingredient in computing self energies accurately, were

extracted from two independent bulk DFT calculations for the three-layer $6 \times 6 \times 1$ Al(111) cells corresponding to the top and bottom electrodes with a single Γ \vec{k}_{\parallel} -point sampling along the electrode-surface direction and a four- \vec{k}_{\perp} -point sampling along the electrode-normal direction. Our calculations for the junction models including up to 684 atoms are one of the largest first-principles MGF studies to date. Although it is possible to treat even mesoscopic-scale junctions by patching channel resistances obtained from thousands of independent small MGF calculations,²⁶ it should be noted that such a scheme cannot be straightforwardly applied to the atomistic junction models that include electrodes as well as the channel itself.

In Fig. 1(b), we show the length scaling of resistances of **open** and **H-end** CNT models, respectively, calculated using the Landauer formula²⁴

$$R = \frac{h}{2e^2} \frac{1}{T(E_F)} = R_Q + \frac{h}{2e^2} \frac{1 - T(E_F)/M}{T(E_F)/M}, \quad (2)$$

where h is the Planck's constant, M is the number of modes ($M=2$ for CNT), $R_Q = h/4e^2 \approx 6.5 \text{ k}\Omega$ is the quantized contact resistance, and the last term is the channel resistance. For CNT junctions with channel length L_{ch} longer than typical scattering lengths, e.g., low-bias mean free path $\Lambda_{\text{mfp}} \sim 200 \text{ nm}$ driven by acoustic phonons, the last term dominates the length scaling and will lead to the linearly increasing resistance $\sim L_{\text{ch}}/\Lambda_{\text{mfp}}$ as required by Ohm's law.^{4,24} However, for our short CNT models, the resistance should instead follow the expression for the tunneling in metal-insulator-metal junctions and scale exponentially according to

$$R = R_0 \exp(\beta L_{\text{ch}}), \quad (3)$$

where R_0 is an effective contact resistance and β is the tunneling growth constant,²⁷ with a minimum resistance of R_Q .

The resistances show the minimum achievable resistance of R_Q at short lengths and rapidly increase with L_{ch} . The most noticeable common feature is the abrupt transition from the large- β to small- β scaling regimes (from 0.38 to 0.11 at 2.7 nm for the **open** model and from 0.52 to 0.16 at 4.7 nm for the **H-end** model). While similar transition behavior was previously observed for some molecular wires,^{28,29} we point out that the physical origin in the two cases is different. In the molecular junction experiments, the long-length scaling is linear and originates from the thermally activated hopping, i.e., the transition results from the change in the charge transport mechanism from coherent tunneling at short lengths to incoherent hopping at long lengths. On the other hand, the long-length scaling in our CNT models also originates from tunneling as the short-length scaling. Indeed, the linear-scale plots of R versus L_{ch} for long CNTs are exponential, as shown in the insets of Fig. 1(b). Therefore, instead of a change in the transport mechanism, the transition corresponds to that from the Schottky-barrier-dominated interface to the CNT-body-dominated intrinsic conductance regimes.

One important quantitative difference between the two scaling curves is the transition length, i.e., 2.7 and 4.7 nm for the **open** and **H-end** models, respectively. The transition length effectively defines (twice) the Schottky barrier width

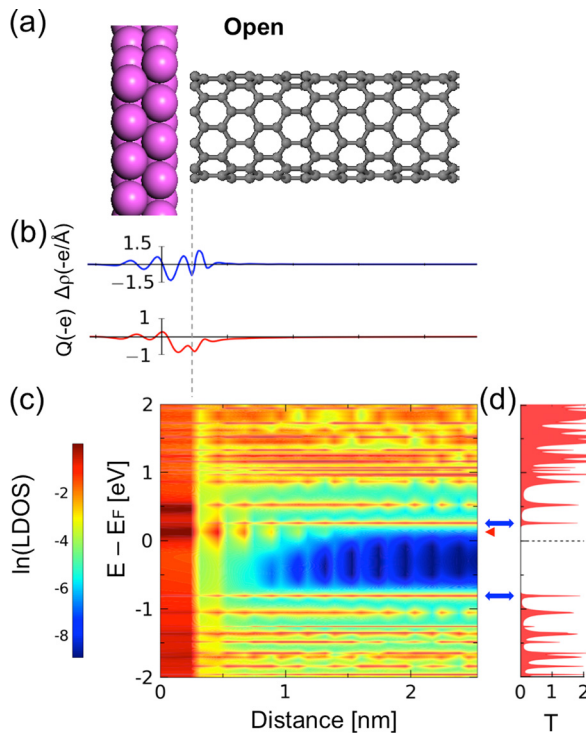


FIG. 2. Structural, electrostatic, electronic, and transport properties of Al(111)-**open** CNT contacts. (a) Side view of the junction model. The corresponding (b) plane-averaged charge density differences at the Al-CNT contact $\Delta\rho$ and its integration Q , (c) LDOS along the channel shown in the log scale, and (d) transmission.

or (twice) the decay length of metal-induced gap states (MIGS) that will be discussed below. Overall, the above difference implies that the Schottky barrier shape (especially width) depends sensitively on the bonding characters of metal-CNT contacts.

In Fig. 1(b), we finally note that the difference in the transition length (or Schottky barrier width) results in the resistance of the **H-end** model (with weak metal-CNT chemical bonds) being lower than that of the **open** model (with strong metal-CNT chemical bonds) for short L_{ch} (below ~ 4.5 nm), which is the *opposite* of the eventual ordering in the long L_{ch} limit. This identifies the origin of the controversy on the metal-CNT bonding strength required for optimal contacts and, more generally, explains the limited relevance of most previous first-principles studies (based on short CNT models and/or without checking the resistance length scaling) for the actual device engineering.

To understand the peculiar length scaling behavior of the two junction models, we now analyze the metal-CNT charge transfer, spatial distribution of energy levels including MIGS, and transmission in detail using the 12-unit **open** and **H-end** CNT models (with L_{ch} of 5.5 nm and 5.7 nm, respectively, i.e., in the long-length regime) as shown in Figs. 2(a) and 3(a), respectively. First, we the plane-averaged real-space charge redistributions resulting from the metal-CNT interaction $\Delta\rho = \rho_{\text{CNT+Al}} - (\rho_{\text{CNT}} + \rho_{\text{Al}})$ and integrated plane-averaged charge density differences $Q(z) = \int_0^z \Delta\rho(z') dz'$ shown in Figs. 2(b) and 3(b) for the **open** and **H-end** models, respectively. A positive (negative) $\Delta\rho$ indicates a gain (loss) in electron density upon the metal-CNT coupling, while a positive (negative) Q indicates a right-to-left (left-to-right) electron transfer. We

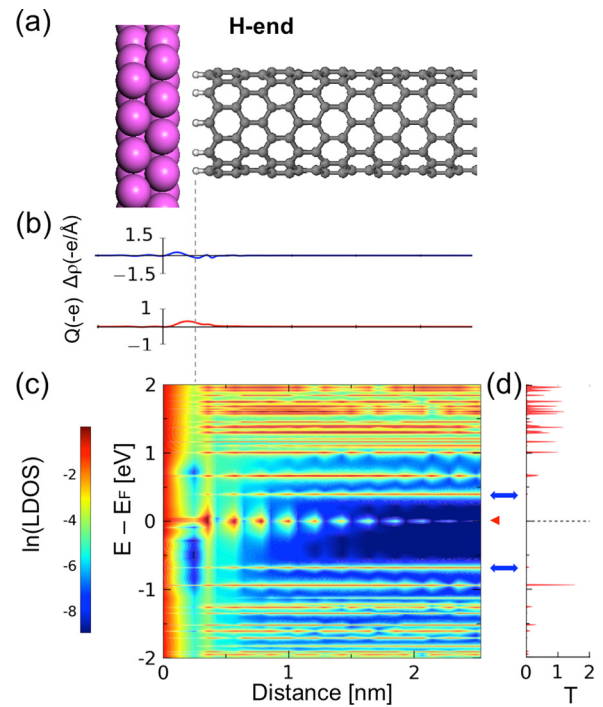


FIG. 3. Structural, electrostatic, electronic, and transport properties of Al(111)-**H-end** CNT contacts. (a) Side view of the junction model. The corresponding (b) plane-averaged charge density differences at the Al-CNT contact $\Delta\rho$ and its integration Q , (c) LDOS along the channel shown in the log scale, and (d) transmission.

observe induced charge redistribution in the **open** model: The net Al-to-CNT charge transfer is the strongest in the interface gap region but also penetrates into the CNT by several angstroms. Meanwhile, for the **H-end** model, much smaller net CNT:H-to-Al electron transfer and its faster decay along the CNT and Al are observed.

The above-described electrostatic information discriminates the **open** and **H-end** models, and, e.g., the significantly smaller resistance of **open** compared with that of **H-end** in the long-length limit can be correlated with the much larger charge transfer in the former. However, the contrasting scaling transitioning behavior, particularly the much smaller resistance of weakly bonded **H-end** in the short-length limits cannot be explained by the amount of charge transfer alone. Therefore, we next examine the energy-level alignment and energy-dependent charge injection properties analyzed by the local density of states (LDOS) and transmission, respectively.

Comparing Figs. 2(c) and 3(c) for **open** and **H-end**, respectively, we note, e.g., the stronger *n*-type (or more downshifted) band alignment of **open** than **H-end** in agreement with the difference in the amount of charge transfer. More importantly, we observe a clear and more microscopic picture that signifies better metal-CNT electronic connectivity in the **open** model than in the **H-end** counterpart; while LDOS around the metal-**H-end** CNT contact regions are distinctively disconnected [Fig. 3(c)], we find more continuous metal-CNT spectra in the metal-**open** interface regions [Fig. 2(c)]. This results in overall much more prominent LDOS and resulting stronger (long-length-limit) transmissions [Figs. 2(d) and 3(d)] not only near the Fermi level E_F but also outside the band edges (indicated by blue double arrows) in **open** than in **H-end**.

The only exception to the above-described comparative features of LDOS spectra result from MIGS (indicated by red left triangles) that are energetically located between the valence and conduction band edges and spatially formed near the metal-CNT contact area and exponentially decay into the CNT body. While the transmissions resulting from these MIGS are negligible for the CNT models in the long-length limit [Figs. 2(d) and 3(d)], they in fact determine the short-length limit resistances [Fig. 1(b)]. Comparing now the **H-end** and **open** models, we find that, in contrast to other states, MIGS LDOS of **H-end** located at E_F are more pronounced than those in **open** that appear below the conduction band edge. Using the **open** model, we have previously pointed out that the strength of these MIGS and associated interface dipole (or the amount of charge transfer) can be stronger for narrower-diameter CNTs.¹² However, the atomic structure of CNT edges is apparently a more important factor in determining the nature of MIGS, which induced the very low contact resistances of the short **H-end** models as observed in Fig. 1(b). To be specific, the origin of MIGS pinned at E_F is the localized states appearing at the hydrogenated edges of graphene sheets.⁹ We note that such localized states also coexist with the dangling bond states at the dehydrogenated pristine graphene edges.¹⁰ However, our data show that although the identity of localized states in the hydrogenated graphene/CNT edges are well-preserved even after the weak bonding with metals, the localized states in the H-free graphene edges more easily lose their characters upon strong metal-graphene/CNT bonding.

In summary, by observing the length scaling of contact resistances obtained from first principles, we have demonstrated the strikingly sensitive dependence of Schottky barrier shape and associated interface dipoles and MIGS on the atomistic details of metal-CNT contacts. We showed that the quality of contacts can be fully understood only by looking into both the long-length limit resistance (transmission curve) and the local chemistry (LDOS plot). Localized states ubiquitous to graphene/CNT edges were identified as an important source of MIGS, which can critically affect the charge injection behavior and result in an anomalous resistance length scaling. The fact that the MIGS decay length can vary substantially according to the atomic structure of metal-CNT contacts and the MIGS-dominated contact region can extend up to ~ 5 nm should have significant implications in realizing sub-10 nm CNT transistors.⁴

This work was supported by the Korea Science and Engineering Foundation (KOSEF, Grant No. 2008-02807) funded by the Ministry of Education, Science and Technology and the National Research Foundation (NRF, Grant No. 2010-0006910).

- ¹S. J. Tans, A. R. M. Verschueren, and C. Dekker, *Nature (London)* **393**, 49 (1998).
- ²R. Martel, T. Schmidt, H. R. Shea, T. Hertel, and P. Avouris, *Appl. Phys. Lett.* **73**, 2447 (1998).
- ³A. Javey, J. Guo, Q. Wang, M. Lundstrom, and H. Dai, *Nature (London)* **424**, 654 (2003).
- ⁴A. D. Franklin, M. Luisier, S.-J. Han, G. Tulevski, C. M. Breslin, L. Gignac, M. S. Lundstrom, and W. Haensch, *Nano Lett.* **12**, 758 (2012).
- ⁵J. Svensson and E. E. B. Campbell, *J. Appl. Phys.* **110**, 111101 (2011).
- ⁶S. Heinze, J. Tersoff, R. Martel, V. Derycke, J. Appenzeller, and P. Avouris, *Phys. Rev. Lett.* **89**, 106801 (2002).
- ⁷Z. Chen, J. Appenzeller, J. Knoch, Y. M. Lin, and P. Avouris, *Nano Lett.* **5**, 1497 (2005).
- ⁸N. Nemeč, D. Tománek, and G. Cuniberti, *Phys. Rev. Lett.* **96**, 076802 (2006).
- ⁹K. Nakada, M. Fujita, G. Dresselhaus, and M. S. Dresselhaus, *Phys. Rev. B* **54**, 17954 (1996).
- ¹⁰T. Kawai, Y. Miyamoto, O. Sugino, and Y. Koga, *Phys. Rev. B* **62**, R16349 (2000).
- ¹¹B. Shan and K. Cho, *Phys. Rev. Lett.* **94**, 236602 (2005).
- ¹²Y.-H. Kim and Y. M. Byun, *J. Korean Phys. Soc.* **55**, 299 (2009).
- ¹³P. Pomorski, C. Roland, and H. Guo, *Phys. Rev. B* **70**, 115408 (2004).
- ¹⁴J. J. Palacios, P. Tarakeshwar, and D. M. Kim, *Phys. Rev. B* **77**, 113403 (2008).
- ¹⁵V. Vitale, A. Curioni, and W. Andreoni, *J. Am. Chem. Soc.* **130**, 5848 (2008).
- ¹⁶B. Shan and K. Cho, *Phys. Rev. B* **70**, 233405 (2004).
- ¹⁷S. Okada and A. Oshiyama, *Phys. Rev. Lett.* **95**, 206804 (2005).
- ¹⁸N. Park and S. Hong, *Phys. Rev. B* **72**, 045408 (2005).
- ¹⁹Y. Matsuda, W. Q. Deng, and W. A. Goddard, *J. Phys. Chem. C* **129**, 11113 (2007).
- ²⁰D. Mann, A. Javey, J. Kong, Q. Wang, and H. J. Dai, *Nano Lett.* **3**, 1541 (2003).
- ²¹Y. Noshu, Y. Ohno, S. Kishimoto, and T. Mizutani, *Jpn. J. Appl. Phys.* **46**, L474 (2007).
- ²²Y.-H. Kim, S. S. Jang, Y. H. Jang, and W. A. Goddard III, *Phys. Rev. Lett.* **94**, 156801 (2005).
- ²³J. P. Perdew, K. Burke, and M. Ernzerhof, *Phys. Rev. Lett.* **77**, 3865 (1996).
- ²⁴S. Datta, *Quantum Transport: Atom to Transistor* (Cambridge University Press, Cambridge, UK, 2005).
- ²⁵Y.-H. Kim, J. Tahir-Kheli, P. A. Schultz, and W. A. Goddard III, *Phys. Rev. B* **73**, 235419 (2006).
- ²⁶Y. S. Lee, M. B. Nardelli, and N. Marzari, *Phys. Rev. Lett.* **95**, 076804 (2005).
- ²⁷J. G. Simmons, *J. Appl. Phys.* **34**, 1793 (1963).
- ²⁸B. Giese, J. Amaudrut, A.-K. Köhler, M. Spormann, and S. Wessely, *Nature (London)* **412**, 318 (2001).
- ²⁹S. H. Choi, B. Kim, and C. D. Frisbie, *Science* **320**, 1482 (2008).